Small H-Shaped Antennas for MMIC Applications

Dilbagh Singh, *Student Member, IEEE*, Christos Kalialakis, *Member, IEEE*, Peter Gardner, *Senior Member, IEEE*, and Peter S. Hall, *Senior Member, IEEE*

***Abstract*—A small short-circuited H-shaped GaAs monolithic microwave integrated circuits (MMICs) patch antenna is presented. Resonant at 5.98 GHz, it is the lowest frequency MMIC patch antenna reported that we are aware of and is intended for short-range communications (e.g., vehicular). Initial experimental and theoretical characterization of the proposed structure has been carried out on soft microstrip substrates. It has been shown that the size of an H-shaped patch antenna can be reduced to as low as one tenth of that of a half wavelength patch antenna resonant at the same frequency, saving valuable substrate space. Resonance frequency, radiation patterns and gain have been investigated. Ground plane truncation effects, which are important for MMIC applications, have been examined using the finite-difference time-domain (FDTD) method.**

***Index Terms*—Electrically small antennas, monolithic microwave integrated circuits (MMICs), printed antennas.**

I. Introduction

CONVENTIONAL microwave active antennas are built using two or more different substrates, for example gallium arsenide (GaAs) for active devices and glass loaded polytetrafluoroethylene (PTFE) for antennas. At higher microwave frequencies, the parasitics of interconnections between devices become significant and degrade the antenna performance. A close integration of active devices with antennas could be achieved by integrating both the devices and the antenna on the same monolithic microwave integrated circuit (MMIC) substrate. The fabrication cost of MMICs depends directly on the substrate area occupied by the circuit. Therefore, the size of the antenna is very important if it is to be integrated with active devices on a GaAs MMIC substrate. Antennas at millimetric frequencies are small and, therefore, they can be fabricated on GaAs substrates at low cost. At microwave frequencies, the antenna size is relatively large and uneconomical to fabricate on a GaAs substrate.

The resonance frequency of a given size antenna can be reduced by using a higher dielectric constant (ε_r) substrate. However, in gallium arsenide MMICs, the designer is constrained to work with dielectric constant of 12.9. Another common technique to reduce the size of a patch antenna is to terminate one of the radiating edges with a short circuit [1]. The antenna is approximately quarter wavelength $(\lambda_g/4)$ long and, therefore, takes approximately half of the substrate space compared to a half-wavelength antenna. The short to ground is made with either a strip or a number of shorting pins. Sanad [2] investigated the effect of changing the number of shorting pins to ground and found the antenna resonant frequency increased by about 2% when a short strip was replaced by shorting posts. The resonant frequency reduced as the number of shorting pins was reduced. The resonance frequency decreased by approximately 3.8% when three shorting pins to ground were used. The resonance frequency of an antenna can also be reduced by covering the patch with a superstrate [3]. A half wavelength H-shaped antenna was investigated by Palanisamy *et al.* [4] for UHF applications. The resonant frequency of the antenna reduced to about half of that of a half-wavelength rectangular patch antenna of the same size.

In this paper, short-circuited H-shaped antennas [5] suitable for MMIC active antenna applications are investigated. The antenna takes a fraction of the substrate area of a conventional half wavelength patch and has a convenient shape enabling the active circuits to be integrated within the antenna, taking no additional substrate area. The investigation of the performance of the antenna was carried out by building a number of antennas with varying dimensions on soft substrate (Section II). The antennas were fully characterized using in house finite-difference time-domain (FDTD) software (Section III) and a commercial Hewlett-Packard Momentum[1] electromagnetic simulator. The change in the resonance frequency of the antenna with its dimension is presented in Section IV. Based on the design data obtained from the soft substrate work, an H-shaped MMIC antenna was fabricated on GaAs substrate at 5.98 GHz (Section V). This antenna is the lowest frequency antenna in MMIC form that we have seen reported in the literature and is intended for short-range communications applications.

II. Antenna Geometry

A quarter wavelength antenna at 5 GHz was built on glass loaded PTFE substrate, which has relative dielectric constant ε_r of 2.2 and substrate thickness of 0.508 mm. The length L of the antenna is 9.5 mm and the width W was arbitrarily chosen to 11 mm. A step in the width was introduced along the length to make the H-shaped short-circuited antenna as shown in Fig. 1. Dimensions W_1, L_1, and L_2 were varied, while keeping the overall size constant; the effect on resonance frequency was also noted. W_1 has a significant effect on the resonance frequency. Therefore, a suitable value for L_1 and L_2 was chosen so that the fields are evenly distributed for an efficient radiation and for feed matching. The lengths L_1 and L_2 were chosen to be

Manuscript received October 23, 1998; revised October 26, 1999. This work was supported by an EPSRC ROPA Award, Reference GR/K63184 and by the School of Electronic and Electrical Engineering, The University of Birmingham.

The authors are with the Communications Engineering Research Group, School of Electronic and Electrical Engineering, The University of Birmingham, Edgbaston, Birmingham, B15 2TT, U.K. (e-mail: P.Gardner@bham.ac.uk).

Publisher Item Identifier S 0018-926X(00)05792-6.

[1]Momentum is a trademark of Hewlett-Packard.

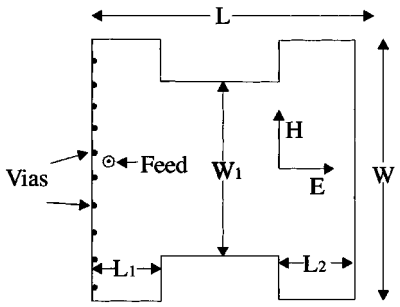

Fig. 1. The layout diagram of short circuit H-shaped antenna.

large enough to set up the radiating fields. At the same time, the central narrow section needed to be long enough to allow its inductance to bring about a worthwhile overall size reduction. The lengths L_1 and L_2 are 2.5 and 2.9 mm, respectively. Ten shorting pins of 0.1 mm thickness were used and the space between the pins was 1 mm. The feed position was determined experimentally such that the return loss was better than -15 dB. The optimum feed position was 1 mm from the shorted end of the patch for the quarter wavelength antenna and 0.8 mm from the shorted end for the Hantennas. The substrate and ground plane size for the antennas was 50 mm $\times$ 50 mm.

III. FDTD Analysis Details

An in-house three-dimensional (3-D) FDTD code was used to analyze the antenna. The H-antenna was modeled using a grid of 161 $\times$ 151 $\times$ 51 cells with spatial resolution $\Delta x = 0.46$ mm, $\Delta y = 0.5$ mm, $\Delta z = 0.17$ mm. The Δz resolution was chosen such that three cells are occupied by the substrate height. The corresponding time step is $\Delta t = 0.5$ ps. Metal parts (antenna, ground plane, and pins) are modeled as perfect electric conductors by setting the tangential electric field components to zero.

Great advantages of the method include wide-band information with a single run and flexibility in geometry. Thus, it is straightforward to model finite ground planes and different dielectrics.

The excitation used is a Gaussian pulse $V_g(t) = \exp[-\alpha(t-\beta\Delta t)^2]$ [6]. The spectrum can be controlled by choosing the constants α, β. For the simulations in this work the values $\beta = 94, \alpha = 0.15 \cdot 10^{23}$ s^{-2} were chosen. Excitation is achieved with a circuit voltage source [7] with internal resistance of 50 Ω to replicate the coaxial probe. This kind of source has been proved to cut down significantly the duration of transients [8].

Radiation patterns can be calculated using a near-to-far field transformation [9]. The time-domain near fields are obtained via sampling on a cuboid transform surface surrounding the antenna. Spatial averaging is required on the transform surface due to the offset of the fields in the FDTD cell. The phasor information at the required frequencies is acquired by performing a running discrete Fourier transform (DFT) along with the simulation. DFT has been proved superior to fast Fourier transform (FFT) when information at few frequencies is needed from FDTD simulations [10]. The field distribution is obtained by sampling the field at a given plane, in this case on the antenna–dielectric interface, and again performing a DFT for

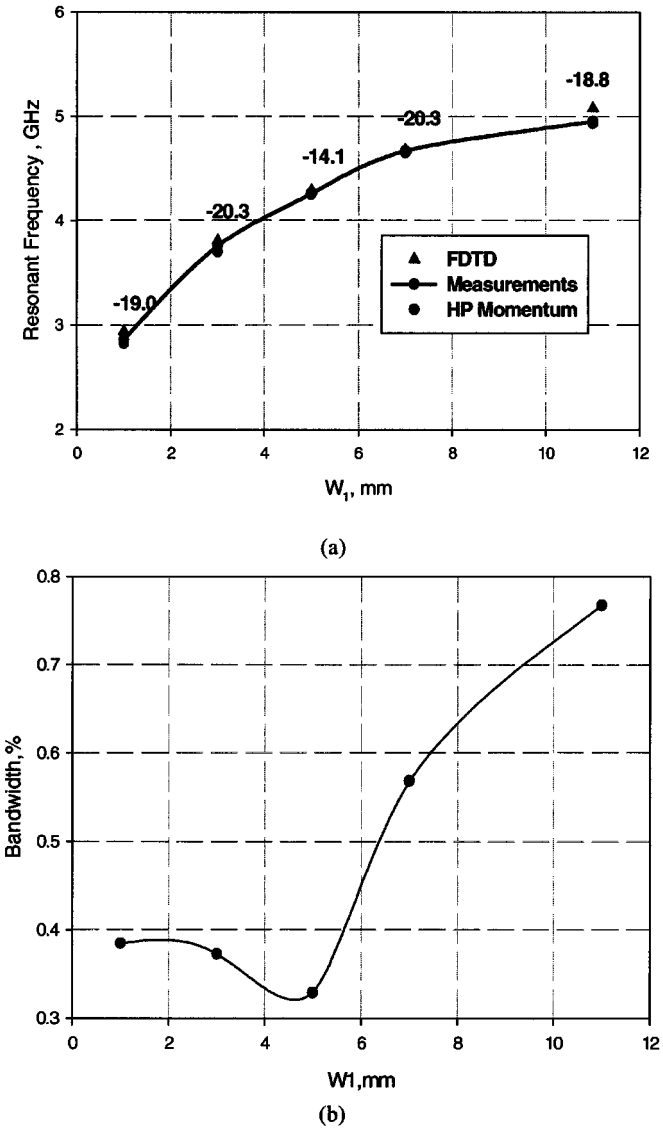

Fig. 2. (a) Measured and simulated resonance frequency of the H-antennas as a function of W_1. The numbers indicate the return loss in decibels at resonance frequency. (b) Measured -10 dB impedance bandwidth ($L = 9.5$ mm, $W = 11$ mm, $L_1 = 2.5$ mm, $L_2 = 2.9$ mm, substrate $\varepsilon_r = 2.2$, and thickness $= 0.508$ mm).

the desired frequency. S_{11} parameters are calculated after the end of the simulation [11] by Fourier transforming the voltage and current time signatures using FFT. Mur second-order absorbing boundary conditions were used [12] except for the corners where first order were used.

IV. Results

In this section, the effect of the width (W_1) on the radiation pattern, resonance frequency, and the antenna field distribution is discussed. The upper limit of the width W_1 is that of a quarter wavelength antenna. Five antennas with middle width (W_1) of 1, 3, 5, 7, and 11 mm were built on soft substrate with geometry as described above in Section II. Radiation patterns, gain, and resonant frequency were measured and simulated. The effect of finite ground plane on the radiation pattern of the antenna is shown both experimentally and by using FDTD. The effect

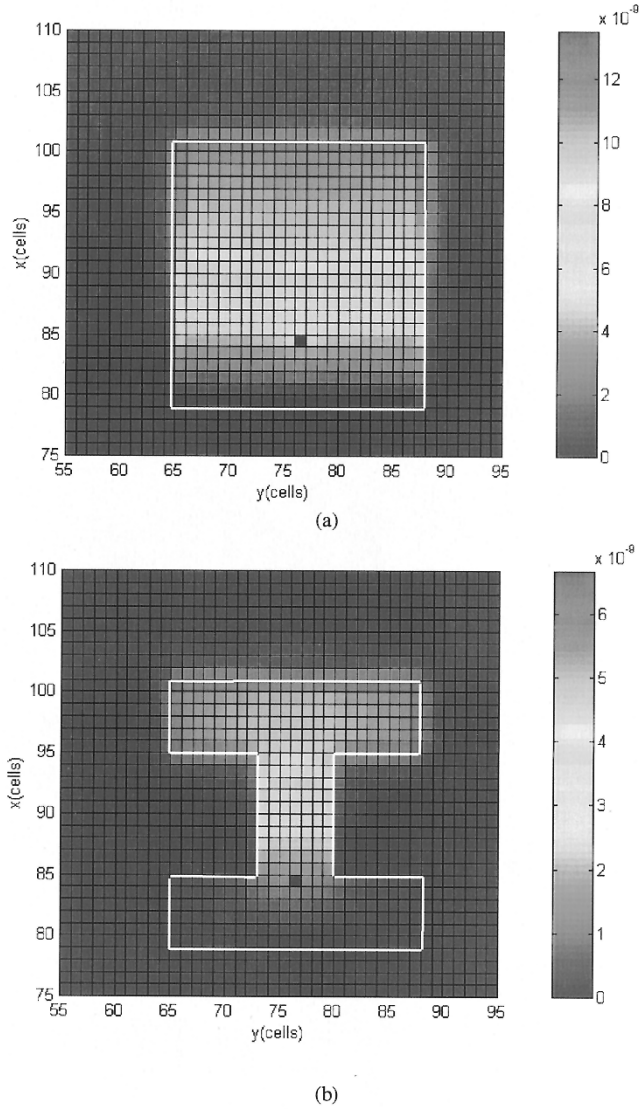

Fig. 3. Calculated electric field distribution. Field calculated using FDTD immediately below patch metallization at the resonance frequency. The patch is outlined in white and the shorted edge is the bottom edge. (a) $W_1 = W$ and (b) $W_1 = 3$ mm (other details as Fig. 2).

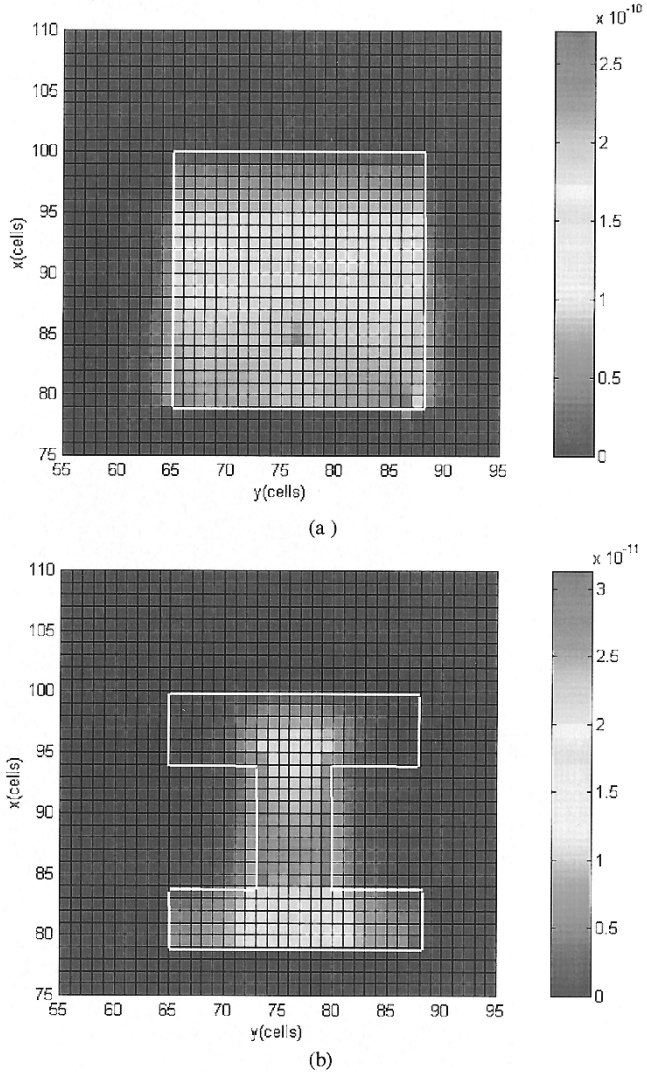

Fig. 4. Calculated current density distribution at the resonance frequency. The patch is outlined in white and the shorted edge is the bottom edge. (a) $W_1 = W$. (b) $W_1 = 3$ mm (other details as Fig. 2).

is especially significant with small W_1, i.e., lower resonance frequencies. The experimental gain of the antenna with different W_1 is also shown together with gain estimations.

A. Resonance Frequency

The middle width W_1 has a significant effect on the resonant frequency of the antenna. Fig. 2 shows the resonance frequency of the H-shaped antenna versus W_1. The resonance frequency is determined by the return loss dip. Experimental results are presented together with results from FDTD and HP momentum. A good agreement has been achieved between experimental results and simulation results giving a maximum error of around 2.5%. It can be seen that the resonance frequency of the antenna reduces by about 42% when the width W_1 is reduced to 1 mm.

B. Fields

The fields were calculated at the resonant frequency using FDTD. Specifically, the electric field component perpendicular to the antenna surface and the surface current density along the length of the patch were calculated. In the case of the electric field the minimum is at the short-circuit edge and the maximum is at the other edge [Fig. 3(a)]. The introduction of a narrow middle section forces the field to conform to the layout. The fringing fields are clearly seen and these should be taken into account when integration is considered [Fig. 3(b)]. Current density reveals the reason why the resonant frequency is lowered. The current density for the quarter wavelength has a peak at the short-circuited side [Fig. 4(a)]. The introduction of the middle section causes a shift of the peak indicating the inductive behavior. The concentration is stronger the narrower the section becomes [Fig. 4(b)]. The field plots give useful insights into the choices of dimensions and the feed location. In Fig. 4(b), the lower current density in the L_1 section gives rise to a slower variation of impedance with feed location. This justifies the choice of a reasonable length L_1, to permit accurate location of the feed. Fig. 3(a) clearly demonstrates the highest E field region near the radiating edge. Fig. 3(b) shows that the choice of L_2 in the H-antenna was appropriate to allow a similar high-field region to be set up.

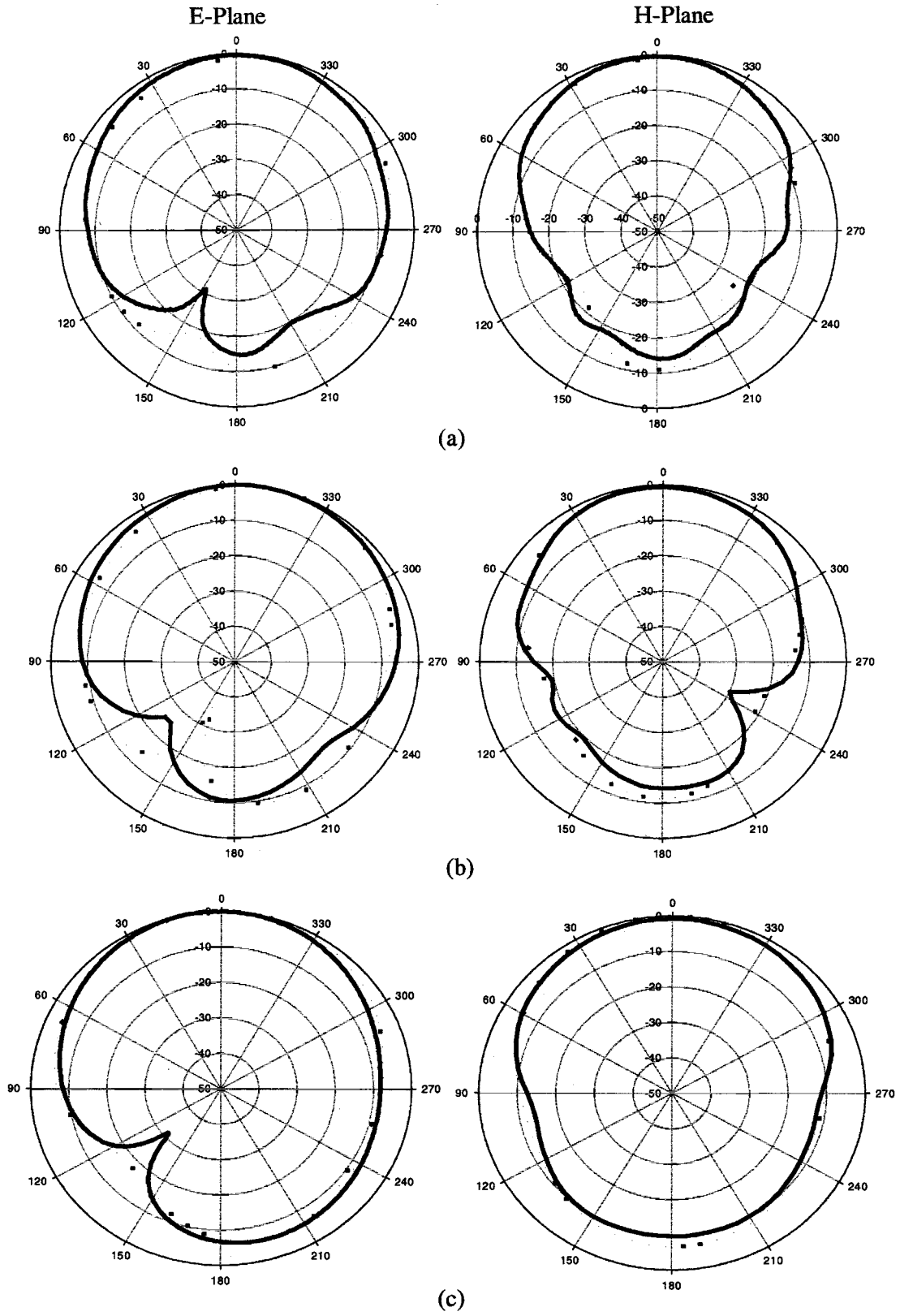

Fig. 5. Radiation patterns (a) quarter wavelength; (b) $W_1 = 3$ mm; and (c) $W_1 = 1$ mm.

C. Radiation Patterns

The E and H plane radiation pattern from experiment and FDTD analysis for three of the five antennas are plotted in Fig. 5. Excellent agreement between experimental and FDTD results is shown for the upper half plane. Good agreement is also obtained for the back lobes which are dependent on the finite ground plane. Very good agreement was also obtained between FDTD

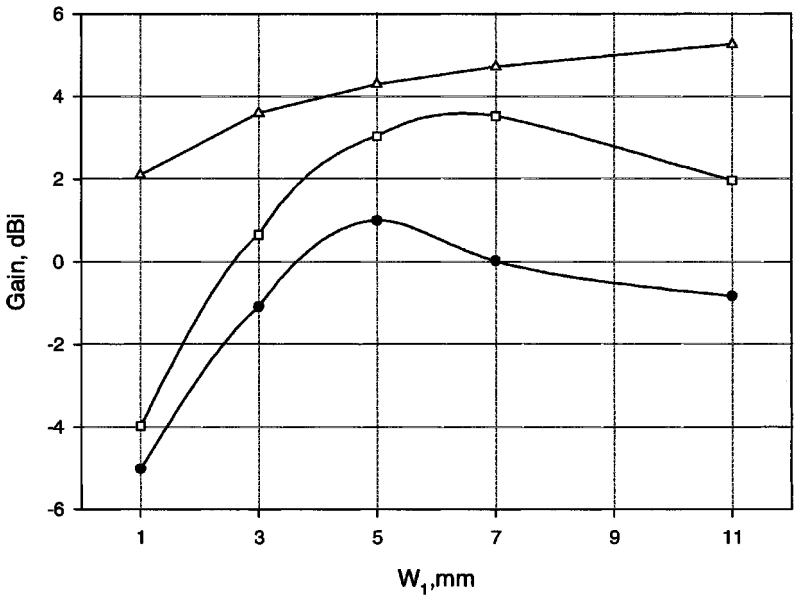

Fig. 6. The measured, maximum realizable, and analytically calculated gains of the H-antennas. (Details as Fig. 2.) Each antenna has been measured/calculated at its resonance frequency.

and experimental results for the other antennas. The worst case cross-polar isolation of all H-shaped antennas tested was 17 dB. The results show that the back lobe of E and H of the antenna increases as the resonance frequency decreases. Since the physical size of the ground plane remained constant for all tested antennas, its electrical length at resonance was reduced as the resonance frequency reduced. In the case when $W_1 = 1$ mm, the resonant frequency is close to 3 GHz and the ground plane length is approximately half a wavelength which explains the almost symmetric back lobe [Fig. 5(c)].

D. Gain of the Antenna

Accurate measurements of the gain of small antennas [13] are very sensitive due to radiation from the feed line or the feeding coaxial cable. In this work, the gains of the antennas at their resonant frequencies were measured by gain comparison using reference dipole antennas with nominal gain of 2.14 dBi. Two dipole antennas with conductor thickness of 0.2 and 0.77 mm that are considered thin wires at the measurement frequencies were used in order to provide a more accurate determination of the gain. The average of the two measurements plotted against W_1 is shown in Fig. 6. The gain at resonance is initially negative, increasing rapidly as W_1 increases, attaining a peak and then gradually dropping off. In order to explain this trend, an estimation of the gain was made based on the electrical size of the antennas.

A rule of thumb for estimating the gain of small antennas is

$$\frac{G \cdot B}{V} = \text{Const} \tag{1}$$

where

G gain of the antenna;
V volume of the antenna;
B bandwidth of the antenna.

This estimate is based on two arguments: the proportionality of bandwidth and volume noted by Balanis for patch antennas [14] and the familiar constant gain bandwidth product from circuit theory. The estimated gain values shown in Fig. 6 are found as follows. The constant is estimated using known gain, bandwidth and volume of a rectangular half-wavelength patch antenna on the same substrate [15] and at the resonance frequency of the H-antenna. The gain of the H-antenna is then found by substituting its volume and measured -10-dB return-loss bandwidth into (1). This is repeated for each of the five H-antennas. The estimated gain is close to the measured values.

It is useful to relate the gain of the proposed antennas to the maximum realisable $(G_{\max})$ of an antenna as given by Harrington [16]

$$G_{\max} = (\beta R)^2 + 2\beta R \tag{2}$$

where R is the radius of the smallest sphere around the antenna. The value for R used was 7 mm. $\beta = (2\pi/\lambda_g)$, where λ_g is the guided wavelength at resonance.

The maximum realisable gain for the antennas of this paper was calculated and plotted in Fig. 6.

A physical explanation for the fact that the resonant gain reaches a peak at an intermediate value of W_1 may be found by considering the power lost to cross-polar radiation. The measured cross-polar isolation on the antenna boresight is high, remaining above 17 dB for all the antennas. However, there are cross-polar sidelobes that account for significantly more power loss. While the main lobe gain initially increases with W_1, the measured level of the peak H-plane cross-polar sidelobes relative to the copolar main lobe, also increase, as shown in Table I. We may estimate a loss factor in decibels arising from power lost to cross-polar radiation as

$$L = 10\log_{10}(1 - I_{\text{xp,max}}) \tag{3}$$

where $I_{\text{xp,max}}$ is the peak cross-polar power divided by the peak main lobe power. This is based on the approximation that the

TABLE I
ESTIMATION OF LOSS DUE TO MEASURED CROSS-POLAR RADIATION

Width of narrow region, W_1, in mm	Measured H-plane cross-polar peak relative to co-polar main lobe: $10\log_{10} I_{xp,max}$	Angle of peak H-plane cross-polar radiation relative to main lobe.	Approximate loss factor $L = 10\log_{10}(1 - I_{xp,max})$
1	-8.0 dB	$\pm 90^0$	-0.7 dB
3	-8.4 dB	$\pm 50^0$	-0.7 dB
5	-6.9 dB	$\pm 65^0$	-1.0 dB
7	-5.9 dB	$\pm 50^0$	-1.3 dB
11	-4.8 dB	$\pm 40^0$	-1.7 dB

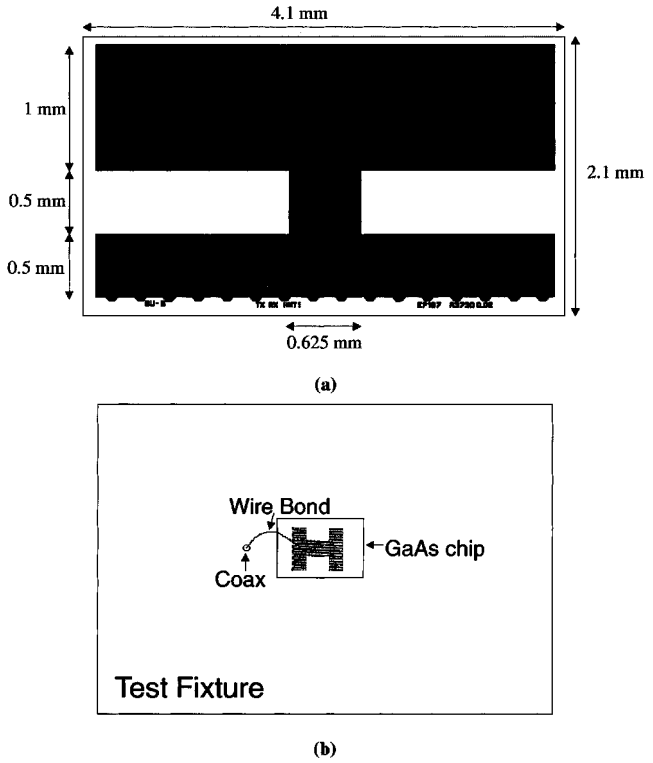

Fig. 7. (a) The layout diagram of MMIC H-antenna. (b) Schematic of test fixture and MMIC chip excitation.

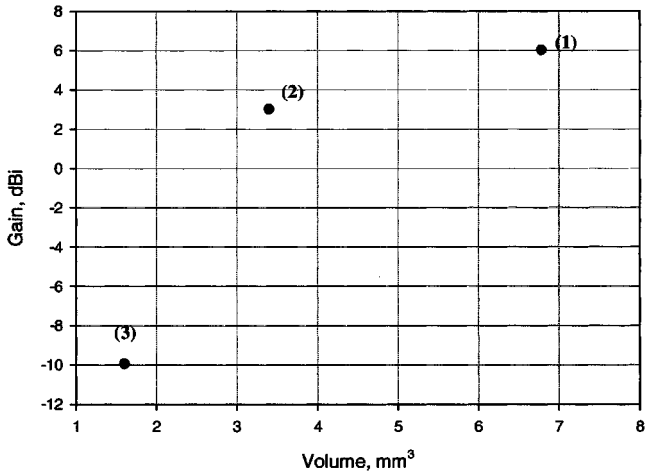

Fig. 8. Estimated gain for GaAs antennas with $\varepsilon_r = 12.9$ and $h = 200\ \mu$m: (1) $\lambda/2$ antenna; (2) $\lambda/4$ antenna; and (3) H-antenna.

total powers in each lobe are in the same proportion as their peak powers.

The loss factor estimated in this way is shown in Table I, indicating an increase of $\sim$1 dB over the range of W_1. Thus, the power lost to cross-polar radiation is of the right order of magnitude to account for the peak in resonant gain at an intermediate value of W_1. The E-plane cross-polar radiation is generally much lower, the worst case being -15 dB relative to the copolar main lobe, for $W_1 = 7$ mm. Power lost to E-plane cross-polar radiation has, therefore, been ignored in this estimate.

V. H-ANTENNA ON GaAs

An H-shaped antenna on a GaAs substrate, based on the design experience described above and shown in Fig. 7(a), was designed for operation at 5.8 GHz. HP Momentum™ software was used for the design since it provides a user friendly interface for MMIC design and mask generation.

The GaAs chip antenna was fabricated using the GEC Marconi F20 MESFET MMIC process. The via holes for the shorted edge of the patch were realized as part of the standard foundry process. The thickness and relative dielectric constant of the MMIC substrate used was 0.2 mm and 12.9, respectively. The overall size of the designed chip was 4.1 mm $\times$ 2.1 mm. The fabricated chips were mounted on a brass chip carrier, as shown schematically in Fig. 7(b). A coaxial connector through the carrier provided the RF feed. The connection from the coaxial

connector to the chip was made via two parallel bondwires to minimize the feed inductance. The optimum feed point on the H-shaped patch was found experimentally.

The experimental resonant frequency of the antenna was 5.98 GHz, 3% different from that computed using HP Momentum™. This discrepancy in the resonance frequency was due to the finite substrate and ground plane of the test fixture (25 mm $\times$ 25 mm). In order to further understand these effects, the FDTD method was used. A grid with $251 \times 131 \times 51$ cells with spatial resolution $\Delta x = 0.1$ mm, $\Delta y = 0.22$ mm, $\Delta z = 0.067$ mm was used. This method gave the resonance frequency of the MMIC antenna as 6.03 GHz, only 0.8% different from the experimental result. The radiation patterns and cross-polar characteristics were found to be very similar to those measured for the soft substrate antennas. The measured gain of the antenna is approximately -9.4 dBi. The estimated gain is -9.9 dBi calculated from (1), using the measured 10-dB return-loss bandwidth of 0.67%. The estimated gains of antennas on GaAs substrates were calculated using (1) and are shown in Fig. 8. The bandwidth of the quarter wavelength antenna was assumed to be the same as that of the half-wavelength antenna.

VI. Conclusion

Small short-circuited H-shaped antennas suitable for MMIC integration have been developed. The resonance frequency of the antenna has been reduced by more than 42% of the same size quarter-wavelength antenna. This antenna takes approximately one tenth of the substrate area of a normal $\lambda/2$ patch antenna resonant at the same frequency. The middle section width is a degree of freedom that could be used by the designer. Gain and resonant frequency design curves have been derived. The radiation patterns calculated and verified are similar to those of a quarter wavelength patch antenna. This antenna will find application where the antenna size is an important constraint—including MMICs. The simple equations given, relating gain, bandwidth, and volume provide an efficient method of estimating the tradeoffs required in potential system applications. Application of the FDTD method provided an accurate tool to account for finite ground plane effects, which are of major importance for MMICs. The limited gain of these small antennas is consistent with the physical limitations derived by Harrington. The reduction in signal could be overcome by integrating an amplifier alongside the narrow central section of the antenna, which would take no extra substrate area on the MMIC. Further reduction in resonant frequency could be achieved by the MMIC package or a glass superstrate in the case of vehicular communications.

References

[1] *Handbook of Microstrip Antennas*, J. R. James and P. S. Hall, Eds., Peter Peregrinus Ltd., London, U.K., 1989.

[2] M. Sanad, "Effect of shorting posts on short circuit microstrip antennas," *IEEE Antennas Propagat. Soc. Symp. Dig.*, pp. 794–797, 1994.

[3] Y. Hwang, Y. P. Zhang, G. X. Zheng, and T. K. C. Lo, "Planar inverted F-antenna loaded with high permittivity material," *Electron. Lett.*, vol. 31, pp. 1710–1712, 1995.

[4] V. Palanisamy and R. Garg, "Rectangular ring and H-shaped microstrip antennas-alternatives to rectangular patch antenna," *Electron. Lett.*, vol. 21, pp. 874–876, 1985.

[5] D. Singh, P. Gardner, and P. S. Hall, "Miniaturised microstrip antenna for MMIC applications," *Electron. Lett.*, vol. 33, pp. 1830–1831, 1997.

[6] K. S. Kunz and R. J. Luebbers, *The Finite Difference Time Domain Method For Electromagnetics*. Orlando, FL: CRC, 1993.

[7] M. Piket-May, A. Taflove, and J. Baron, "FDTD modeling of digital signal propagation in 3-D circuits with passive and active loads," *IEEE Trans. Microwave Theory Tech.*, vol. 42, pp. 1514–1523, Aug. 1994.

[8] R. J. Luebbers and H. S. Langdon, "A simple feed model that reduces time steps needed for fdtd antenna and microstrip calculations," *IEEE Trans. Antennas Propagat.*, vol. 44, pp. 1000–1005, July 1996.

[9] R. J. Luebbers, K. S. Kunz, M. Schneider, and F. Hunsberger, "A finite difference time domain near-zone to far-zone transformation," *IEEE Trans. Antennas Propagat.*, vol. 39, pp. 429–433, Apr. 1991.

[10] C. M. Furse and O. P. Gandhi, "Why the DFT is faster than the FFT for FDTD time-to-frequency domain conversions," *IEEE Microwave Guided Wave Lett.*, vol. 6, pp. 326–328, Oct. 1995.

[11] O. P. M. Pekonen, J. Xu, and K. I. Nikoskinen, "Rigorous analysis of circuit parameter extraction from an FDTD simulation excited with a resistive voltage source," *Microwave Opt. Technol. Lett.*, vol. 12, pp. 205–210, 1996.

[12] G. Mur, "Absorbing boundary conditions for the finite difference approximation of the time domain electromagnetic field equations," *IEEE Trans. Electromagn. Compat.*, vol. EMC-23, pp. 377–382, Nov. 1981.

[13] O. Staub, J. F. Zurcher, and A. Skrivervik, "Some considerations on the correct measurement of the gain and bandwidth of electrically small antennas," *Microwave Opt. Technol. Lett.*, vol. 17, pp. 156–160, 1998.

[14] C. A. Balanis, "Microstrip antennas," in *Antenna Theory: Analysis and Design*. New York: Wiley, 1997, ch. 14.

[15] J. R. James, P. S. Hall, and C. Wood, *Microstrip Antennas—Theory and Design*. London, U.K.: Peter Peregrinus Ltd., 1981, p. 81.

[16] R. F. Harrington, "Effect of antenna size on gain, bandwidth and efficiency," *J. Res. Nat. Bureau Standards—D. Radio Propagat.*, vol. 64D, pp. 1–12, 1960.

Dilbagh Singh (S'97) was born Punjab, India in 1971. He received the degree in electrical and electronics engineering from the University of East London, U.K., in 1995, and the Ph.D. degree from The University of Birmingham, U.K., in 1999.

From 1996, he was Research Associate and worked on active monolithic active microwave and millimeter wave antennas for two years. In 1998, he started at Roke Manor Research Limited as a Microwave Design Engineer. Currently, he is working with Samsung Electronics Research Institute as a Senior RF Engineer. His interests are active antennas and microwave- and millimeter-wave circuits.

Christos Kalialakis (S'94–M'99) was born in Watrellos, France, in 1971. He received the Ph.D. degree in electronic and electrical engineering from the University of Birmingham, U.K., in 1999, and the B.Sc. (physics) and the Master's (telecommunications) degrees from the Aristotle University of Thessaloniki (A.U.Th.), Greece, in 1993 and 1995, respectively.

In 1993, he was an undergraduate research Assistant at the Department of Physics, A.U.Th., working on theoretical solid-state physics. From 1996 to 1998 he served as a Postgraduate Teaching Assistant at the School of Electronic Engineering, University of Birmingham. Since November 1998 he has been employed as a Research Associate working on an industry sponsored project on satellite communications. His research interests include computational electromagnetics, active integrated antennas, and performance evaluation of mobile communications systems.

Dr. Kalialakis is an associate member of the Institute of Electrical Engineers (IEE) and a graduate member of the Institute of Physics, London, U.K..

Peter Gardner (M'99–SM'00) received the B.A. degree in physics from the University of Oxford, U.K., in 1980, and the M.Sc. and Ph.D. degrees in electronic engineering from University of Manchester Institute of Science and Technology (UMIST), Manchester, U.K., in 1990 and 1992, respectively.

From 1981 to 1987, he worked for Ferranti, Poynton, Cheshire, as a Senior Engineer in microwave amplifier development. From 1987 to 1989, he freelanced in microwave engineering and software. In 1989, he joined the Department of Electrical Engineering and Electronics, UMIST, as a Research Associate, where he carried out research in microwave negative resistance circuits, low noise MMIC design, and tunable planar resonators. In 1994, he was a Lecturer in the School of Electronic and Electrical Engineering, University of Birmingham, U.K. His current research interests are in the areas of microwave solid-state component design, active antennas, and amplifier linearization.

Peter S. Hall (M'88–SM'93) received the Ph.D. degree in antenna measurements from Sheffield University, U.K., in 1973.

He is Professor of Communications Engineering, Head of the Communications Engineering Group, and Head of the School of Electronic and Electrical Engineering, University of Birmingham, U.K. He spent three years with Marconi Space and Defence Systems, Stanmore, U.K., working largely on a European Communications Satellite project. He then joined The Royal Military College of Science as a Senior Research Scientist, progressing to Reader in Electromagnetics. He joined The University of Birmingham in 1994. He has researched extensively in the areas of microwave antennas and associated components and antenna measurements. He has published four books, over 130 learned papers, and has various patents. He was honorary editor of *IEE Proceedings Part H Journal* from 1991 to 1995 and is currently on the editorial board of the *International Journal of RF and Microwave Computer Aided Engineering* and *Microwave and Optical Technology Letters*.

Prof. Hall's publications have earned six IEE premium awards, including the 1990 IEE Rayleigh Book Award for the *Handbook of Microstrip Antennas*. He is a Fellow of the IEE and a past Chairman of the IEE Antennas and Propagation Professional Group and of the organizing committee of the 1997 IEE International Conference on Antennas and Propagation. He has been associated with the organization of many international conferences and is currently a member of the technical committee of AP-2000 in Switzerland and is an overseas corresponding member of ISAP2000 in Japan.